REFERENCES

[1] A. Khebir, A. Kouki, and R. Mittra, "Asymptotic boundary conditions for finite element analysis of three dimensional line discontinuities," *IEEE Trans. Microwave Theory Tech.*, vol. 38, no. 10, pp. 1427–1432, 1990.

[2] F. R. Cooray and G. I. Costache, "An overview of the absorbing boundary conditions," *J. Electromagn. Waves Appl.*, vol. 5, no. 10, pp. 1041–1054, 1991.

[3] S. Pissanetzky, "A simple infinite element," *COMPEL-Int. J. Comput. Math. Elect. Eng.*, vol. 3, no. 2, pp. 107–114, 1984.

[4] A. Khebir and A. B. Kouki, "Higher order asymptotic boundary condition for the finite element modeling of two-dimensional transmission line structures," *IEEE Trans. Microwave Theory Tech.*, vol. 38, pp. 1433–1438, 1990.

[5] P. P. Silvester and R. L. Ferrari, *Finite Elements for Electrical Engineers*, 2nd ed. Cambridge: Cambridge Univ. Press, 1990.

[6] W. T. Weeks, "Calculation of coefficients of capacitance of multiconductor transmission lines in presence of a dielectric interface," *IEEE Trans. Microwave Theory Tech.*, vol. 18, pp. 35–43, 1970.

Thru Characteristics of a Coaxial Gap (FDTD Model and Measurements)

Bruce G. Colpitts

***Abstract*—Thru characteristics of a coaxial cable interrupted by a small gap are modeled and measured. Finite-difference time-domain (FDTD) modeling is applied in cylindrical coordinates to semirigid coaxial cable and to the intervening gap material. Both dispersive and nondispersive gap materials are investigated. Gap loss and phase shift are accurately predicted by this two-dimensional model which accounts for TEM and TM modes in the gap and coaxial apertures. An application of the model is to establish reference data for thin sample permittivity or moisture measurements.**

I. INTRODUCTION

A FDTD model in cylindrical coordinates is presented for a coaxial cable and intervening small gap. That is the cable is severed and a gap of up to one probe diameter (3.58 mm) is opened between the ends. Modeled results are verified with measurements to demonstrate accuracy for several gap sizes and materials. The coaxial gap is proposed as a sensor for very localized permittivity measurements of thin samples as an alternative to the coaxial reflection method which requires stacking of thin samples [1], [2] or the semiempirical approach used in [2] which requires two measurements of the same sample. Neither method is suitable for continuous thin sample moisture measurement. Since FDTD results are not readily invertible the procedure for determination of permittivity would be to characterize the gap response for a number of materials or moisture levels as part of calibration and to then use an interpolation procedure to determine the actual permittivity from the measured values. With sufficient computational speed an iterative solver would be feasible. This paper presents the FDTD numerical model along with measurements of two thin samples for verification. This presentation deals with the transmission response of the gap while in [3] the reflection properties of the coaxial cable have been considered and found to be accurately predicted by this approach. Now with the reflection and transmission properties well modeled and through the use of [4] one can either iteratively or through a look-up procedure determine the material properties.

Manuscript received September 6, 1994; revised October 2, 1995.

The author is with the Department of Electrical Engineering, University of New Brunswick, Fredericton, NB, Canada.

Publisher Item Identifier S 0018-9480(96)00462-0.

II. NUMERICAL ANALYSIS

A lossless and nondispersive cable dielectric is assumed while the gap material may have loss and dispersive characteristics. Dispersion is accounted for through recursive relations similar to those in [5]. The model is two-dimensional with the center of the center conductor forming a line of symmetry as in Fig. 1. This two-dimensional model accounts for TEM and TM modes at the apertures and throughout the gap but is not capable of modeling TE modes. This is not expected to be a limiting factor since the actual problem has circular symmetry and thus there are no mechanisms to excite TE modes [6]. Due to the small cable size chosen for this study and the need to precisely model gap details a cell size of 0.2 mm is chosen. This yields 52 cells from the inner conductor to the outer conductor in 3.58 mm (0.141") cable or 392 cells per wavelength at 26.5 GHz. With this small element size the Courant condition requires a correspondingly small time step, in the tens of picosecond range, depending upon the dielectric material selected. Field components used in this solution are the axial and radial electric fields and the circumferential magnetic field. Absorbing boundaries are of the first order Mur [7] type applied to the axial electric field while the line of symmetry is accounted for through symmetry of the magnetic field. Governing field equations in cylindrical coordinates are given in pseudo code form below for dispersive materials where the Debye equation and an additional conductivity term are used to describe their frequency dependent behavior as follows

$$\epsilon^*(\omega) = \epsilon_\infty + \frac{\epsilon_S - \epsilon_\infty}{1 + j\omega\tau_0} - j\frac{\sigma}{\omega\epsilon_0}. \tag{1}$$

Where the terms are defined as follows with their corresponding values for water at 25° shown in brackets, ϵ_∞ = permittivity at infinite frequency (4.9), ϵ_S= static permittivity (78.52), τ_0 = relaxation time (8.38×10^{-12}), σ = conductivity (0.0), and ω = angular frequency

$$HC^{n+1/2}(I,J) = HC^{n-1/2}(I,J) + F^*((EA^n(I+1,J) - EA^n(I,J)) - (ER^n(I,J+1) - ER^n(I,J)) \tag{2}$$

$$ER^{n+1}(I,J) = B^*ER^n(I,J) + C^*(HC^{n+1/2}(I,J-1) - HC^{n+1/2}(I,J)) + D^*SR^n(I,J) \tag{3}$$

$$SR^{n+1}(I,J) = A^*SR^n(I,J) + 0.5^*(A^*ER^n(I,J) + ER^{n+1}(I,J)) \tag{4}$$

$$EA^{n+1}(I,J) = B^*EA^n(I,J) + E^*(HC^{n+1/2}(I,J) - HC^{n+1/2}(I-1,J)) + C^*(HC(I,J) - HC(I-1,J)) + D^*SA^n(I,J) \tag{5}$$

$$SA^{n+1}(I,J) = A^*SA^n(I,J) + 0.5^*(A^*EA^n(I,J) + EA^{n+1}(I,J)) \tag{6}$$

where EA = axial electric field, ER = radial electric field, HC = circumferential magnetic field, SR = recursive radial term, SA = recursive axial term

$$A = e^{-(\Delta t/\tau_0)} \tag{7}$$

$$B = 1 - \Delta t^*(\sigma/(\epsilon^*_\infty \epsilon_0) + (\epsilon_S - \epsilon_\infty)/(\epsilon^*_\infty \tau_0), \tag{8}$$

$$C = \Delta t/(\epsilon^*_0 \epsilon^*_\infty \Delta), \tag{9}$$

$$D = (\epsilon_S - \epsilon_\infty)/\epsilon^*_\infty (\Delta t/\tau_0)^2, \tag{10}$$

$$E = C^*0.5^*Radius^*\Delta, \tag{11}$$

$$F = \Delta t/(\mu^*_0 \Delta), \tag{12}$$

Δt = time step, Δ = grid size, μ_0= permeability of free space, and ϵ_0 = permittivity of free space. The coaxial inner and outer conductors are modeled as perfect conductors by forcing the surface tangential electric field to zero. Circular symmetry allows the gap axial electric field to be determined from

$$EA^{n+1} = EA^n + \Delta t/(\epsilon + \sigma \Delta t)\Delta^*(2^*HC^{n+1/2}) \tag{13}$$

along the line of symmetry.

The two cable end configurations considered are shown in Fig. 1 where (a) shows the cable aperture in an infinite ground plane or flange while (b) is a cable with no ground plane referred to as the flangeless case. Both cases are modeled and compared with measurements in following sections.

A Gaussian pulse is used to excite the cable. This pulse propagates to the gap where a reflection occurs dividing the energy between a reflected pulse and one that propagates into the gap. Of the energy entering the gap some is absorbed in the gap material, some is radiated, and a portion enters the second cable. In this model both reflected and transmitted voltage pulses can be determined and used to define the gap scattering parameters. Sampling of the fields occurs away from the apertures to avoid higher order TM modes excited by the aperture discontinuities. For reflection measurements sufficient distance between the sample point and aperture is used in order to separate incident and reflected fields in the time domain. Although the fields are sampled away from the aperture for the above reasons they are translated back to the aperture using theoretical cable propagation velocities. Thus the loss and phase shift results are for the gap only. This data is taken into a numerical mathematics package where both input and output are Fourier transformed to the frequency domain. The ratio of output to input voltage is then taken for each frequency point which yields both amplitude and phase information. Data presented here extends to 26.5 GHz which corresponds to the experimental frequency limit although with the small cell size used in the model much higher frequencies could be analyzed.

III. Measurement Procedure

A coaxial gap was created by mounting two 3.58 mm semirigid coaxial cables in a precision carriage which allows the cables to be forced together for calibration and then separated by a known distance. The cables are carefully aligned in order that they remain on the same axis as they are separated while the distance is measured with a dial micrometer having 0.01 mm resolution. Prior to mounting, the cable faces are machined perpendicular to the cable axis and polished to ensure a flat clean surface to mate with the opposing cable. These cables are both flangless and during measurement the air or

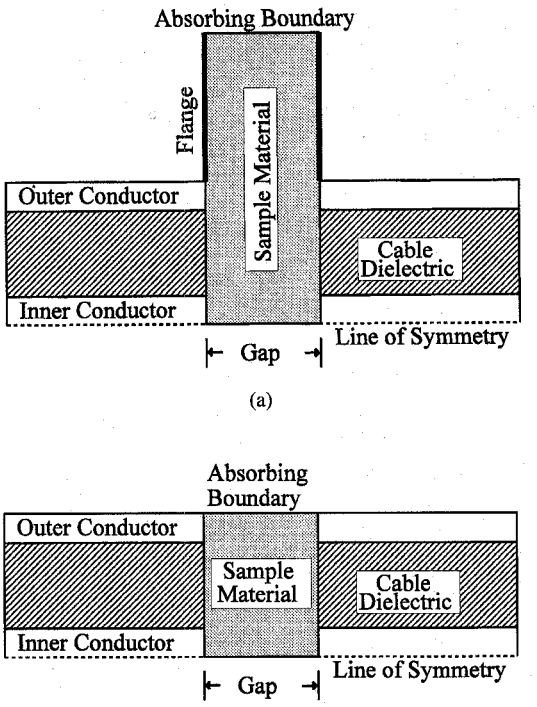

Fig. 1. (a). Cross sectional view of the flanged coaxial probes and intervening gap. (b). Cross sectional view of the flangeless coaxial probes and intervening gap.

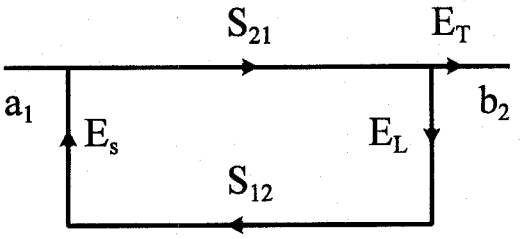

Fig. 2. Scattering model of the coaxial gap under calibration conditions (probes forced together).

water completely engulfs the gap and surrounding region. A reference is established by forcing the two cables together and measuring the thru characteristics. This is necessary since calibration standards are not available to apply directly to cable ends. A simple error model for this situation is given in Fig. 2 where S_{11} and S_{22} approach zero while S_{21} and S_{12} approach unity, this occurs as the cable junction becomes transparent. Error terms in the model include E_T which is the transmission response coefficient accounting for attenuation and delay in the cables and connectors while E_S and E_L are source and load match error terms. Transmission response is the dominant error with the match terms primarily associated with connector mismatch contributing secondary effects. The circuit of Fig. 2 yields a response

$$\frac{b_2}{a_1} = \frac{E_T}{1 - E_L E_S} \tag{14}$$

where the match terms produce a rapidly varying response in the frequency domain and in this broadband application these effects can be filtered out. When the cables are separated S_{11} and S_{22} now approach unity since most of the energy is reflected and S_{12} and S_{21} are greatly reduced. This situation is represented by the error model of Fig. 3 where coupling across the gap is small enough to ignore

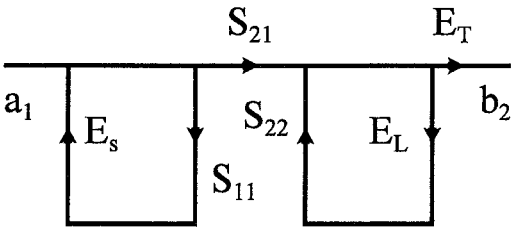

Fig. 3. Scattering model of the coaxial gap when probes are separated.

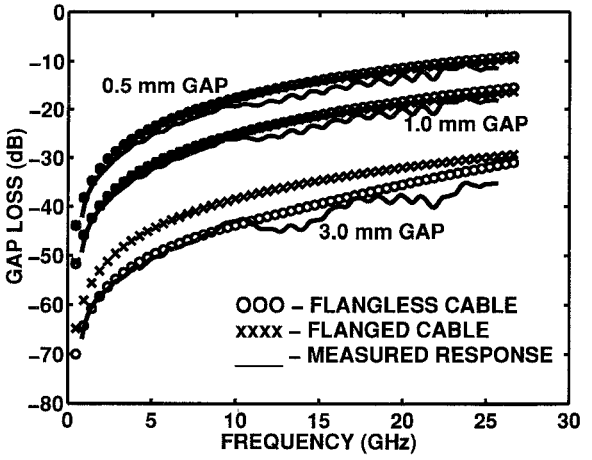

(a)

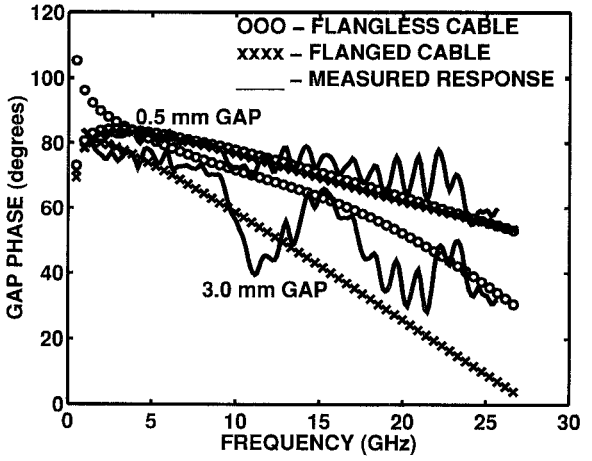

(b)

Fig. 4. Measured and computed attenuation (a) and phase shift (b) resulting from air filled gaps of 0.5 mm, 1.0 mm and 3.0 mm being introduced into a coaxial cable.

multiple traverses and the errors needing consideration are again transmission response, and load and source match. This situation gives a system response as follows:

$$\frac{b_2}{a_1} = S_{21}\frac{E_T}{(1 - S_{11}E_S) * (1 - S_{22}E_L)}. \tag{15}$$

A periodic variation in the frequency response results from connector mismatch which appears in the load and source match error terms. This ripple rate is proportional to the spacing between gap and connector which in this case is approximately 8 cm of Teflon dielectric cable. Assuming that the magnitudes of S_{11}, S_{22}, E_S, and E_L vary slowly with frequency compared to the phase of the

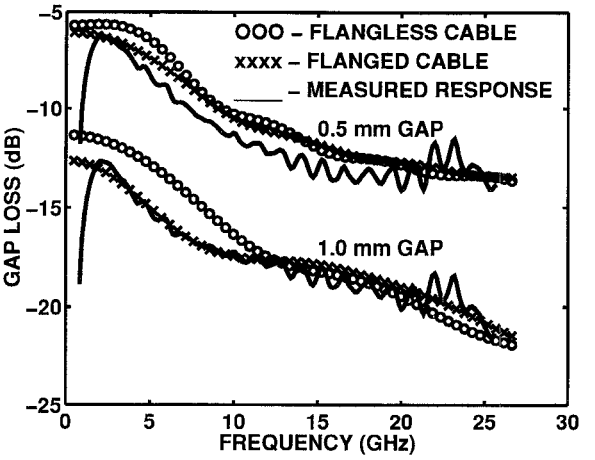

(a)

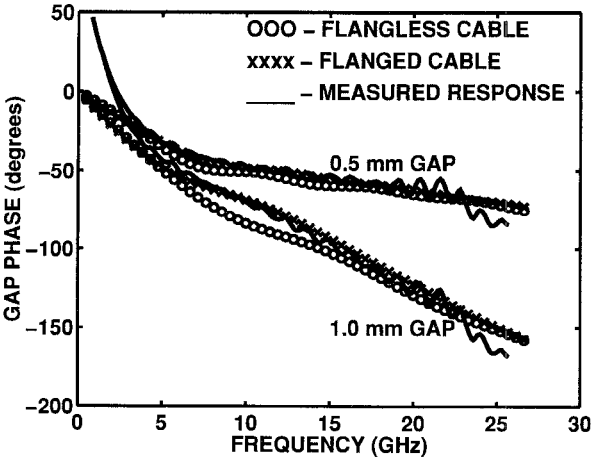

(b)

Fig. 5. Measured and computed attenuation (a) and phase shift (b) resulting from water filled gaps of 0.5 mm and 1.0 mm being introduced into a coaxial cable.

match errors then the match errors can be removed through filtering. Application of filtering is appropriate in cases where the device under test has no rapid variation in response with frequency and the measurement is broadband. This method would not be appropriate for narrowband measurements where a more sophisticated error model would be required. Use of open and short circuit terminations on the coaxial cable would be possible in addition to the thru measurement for a more detailed calibration. Measurements were made of air and water at several thicknesses in order to verify numerical model accuracy.

IV. Comparison of Modeled and Measured Results

Presented here are loss and phase shift results associated with a coaxial gap filled with either air or water ranging in thickness from 0.5 mm to 3.0 mm. Both measured and computed results are presented in order to demonstrate model validity.

Fig. 4 presents the results of an air gap in the cable. Part (a) shows loss associated with the gap where good agreement is seen for 0.5 and 1.0 mm gaps both with and without flanges while in the 3 mm case the flange provides a significant improvement. These differing results are caused primarily by the absorbing boundary location in the two cases as in Fig. 1. Without the flange an absorbing boundary is

located at a radial distance corresponding to the outside of the outer conductor which for the 3 mm gap case does not account properly for the field components in that region. Reactive field components associated with the open circuit are not properly accounted for by the absorbing boundary and introduce errors in the model. These errors increase as the gap width increases since a larger portion of the transmitted energy interacts with this nearby absorbing boundary. Fig. 4(b) shows the phase associated with the gap where 0.5 and 1.0 mm results are nearly identical and the 3.0 mm results are distinctly different with a larger error between computed and measured results. In the phase results there is no clear advantage to modeling with or without the flange.

Fig. 5 presents the case for the gap filled with distilled water for both 0.5 mm and 1.0 mm gaps. Good agreement is seen for both loss and phase data of this dispersive liquid. A comparison of with and without flange computations reveals the flangeless case to yield results closer to the measured results as opposed to the air results. This is attributed to the flangeless model being a closer approximation to the actual probe and the much higher dielectric constant of water results in the reactive fields remaining near the aperture so the effects of the absorbing boundary at the outer conductor have little influence here as compared with air.

V. Conclusion

A FDTD model for the coaxial gap filled with both dispersive and nondispersive materials was developed for the coaxial cable with and without a flange at the aperture. Computed results were compared with measurements and found to be in good agreement for both gap loss and phase shift. The FDTD method using standard and recursive relations is seen to accurately predict phase and amplitude behavior of the coaxial gap. Placement of absorbing boundaries is seen to be critical in the coaxial probe model and results in a tradeoff between keeping the computational space small for efficiency and placing absorbing boundaries away from reactive fields for accuracy. As the dielectric constant and loss in the gap material increases there is a reduced requirement on the radial dimension of the model.

References

[1] B. G. Colpitts, Y. Pelletier, and S. R. Cogswell, "Complex permittivity measurements of the colorado potato beetle using coaxial probe techniques," *J. Microwave Power Electromagn. Energy*, vol. 27, no. 3, pp. 175–182. 1992.

[2] M. A. El Rayes and F. T. Ulaby, "Microwave dielectric spectrum of vegetation part I: Experimental observations," *IEEE Trans. Geosci. Remote Sensing*, vol. GE-25, no. 5, pp. 541–549, Sept. 1987.

[3] B. G. Colpitts and J. S. Ployer, "Finite difference time domain model of a coaxial probe: Symp. antenna technology and appl. electromagn.," ANTEM '94, pp. 357–361, Aug. 1994.

[4] J. B. Jarvis, E. J. Vanzura, and W. A. Kissick, "Improved technique for determining complex permittivity with the transmission/reflection method," *IEEE Trans. Microwave Theory Tech.*, vol. MTT–38, no. 8, Aug. 1990.

[5] K. S. Knuz and R. J. Luebbers. *The Finite Difference Time Domain Method for Electromagnetics*. Boca Raton, FL: CRC Press, 1993, pp. 124–131.

[6] J. R. Mosig, J. C. E. Besson, M. G. Fabry, and F. E. Gardiol, "Reflection of an open ended coaxial line and application to nondestructive measurement of materials," *IEEE Trans. Instrum. Meas.*, vol. IM–30, no. 1, pp. 46–51, Mar. 1981.

[7] G. Mur, "Absorbing boundary conditions for the finite difference approximation of the time domain electromagnetic field equations," *IEEE Trans. Electromag. Compat.*, vol. EMC-23, no. 4, pp. 377–382, Nov. 1981.